AD-A284 065

①

Screening of Charged Electrodes in Aqueous Electrolytes

by

DTIC
ELECTE
SEP 0 6 1994
G

Michael R. Philpott
James N. Glosli*

Prepared for publication for

Journal Electrochemical Society Letters

August 29th, 1994

*Lawrence Livermore National Laboratory,
University of California, Livermore, CA 94550

94-28976

REPORT DOCUMENTATION PAGE		READ INSTRUCTIONS BEFORE COMPLETING FORM
1 REPORT NUMBER 10	2. GOVT ACCESSION NO.	3 RECIPIENT'S CATALOG NUMBER
4 TITLE*(and Subtitle)* Screening of Charged Electrodes in Aqueous Electrolytes		5. TYPE OF REPORT & PERIOD COVERED Technical Report
		6 PERFORMING ORG. REPORT NUMBER
7 AUTHOR(s) Michael R. Philpott and James N. Glosli		8. CONTRACT OR GRANT NUMBER(s) N00014-92-C-0173
9 PERFORMING ORGANIZATION NAME AND ADDRESS IBM Research Division, Almaden Research Center, 650 Harry Road San Jose, CA 95120-6099		10 PROGRAM ELEMENT. PROJECT. TASK AREA & WORK UNIT NUMBERS
11 CONTROLLING OFFICE NAME AND ADDRESS Office of Naval Research 800 North Quincy Street Arlington, VA 22217		12 REPORT DATE August 29, 1994
		13. NUMBER OF PAGES 10
14. MONITORING AGENCY NAME & ADDRESS*(If different from Controlling Office)* Dr. Robert J. Nowak Office of Naval Research, Chemistry Division		15. SECURITY CLASS*(of this report)* unclassified
		15a. DECLASSIFICATION/DOWNGRADING SCHEDULE
16 DISTRIBUTION STATEMENT*(of this Report)* Approved for public release; distribution unlimited.		
17 DISTRIBUTION STATEMENT*(of the abstract entered in Block 20, if different from Report)*		
18 SUPPLEMENTARY NOTES		
19 KEY WORDS*(Continue on reverse side if necessary and identify by block number)*		
20 ABSTRACT*(Continue on reverse side if necessary and identify by block number)* see next page		

SCREENING OF CHARGED ELECTRODES IN AQUEOUS ELECTROLYTES

Michael R. Philpott
IBM Research Division, Almaden Research Center,
650 Harry Road, San Jose, CA 95120-6099
and
James N. Glosli
Lawrence Livermore National Laboratory,
University of California, Livermore, CA 94550

Abstract

Molecular dynamics simulations are used to demonstrate for the first time that systems about 4 nm thick containing 1200 to 1600 water molecules and NaCl at 1M to 3M concentrations exhibit the main components of electric double layers at charged metal surfaces. In particular for the system chosen there are regions clearly identifiable as a bulk electrolyte zone, a diffuse layer that screens the charge on the electrode and a layer of oriented water localized next to the electrode. The width of the diffuse layer increases with decrease in salt concentration from 0.2 nm at 3 M to 0.5 nm at 1 M. All the calculations are based on the simple point charge model (SPCE) water model and the immersed electrode approximation.

Accesion For		
NTIS CRA&I		X
DTIC TAB		☐
Unannounced		☐
Justification		
By		
Distribution /		
Availability Codes		
Dist	Avail and / or Special	
A-1		

INTRODUCTION

Electric double layers are some of the basic organ... ...or- ...lopted in electrochemical and biological systems to shield fields arising from layers and an 's of charge in contiguous structures. It is therefore quite important to understand their properties using simple models without introducing further approximations. In this letter we describe the first molecular dynamics simulation of a complete electric double layer and detail it's structure from the charged surface of the metal electrode all the way to the bulk electrolyte zone, in terms of water and ion time independent probability distribution functions averaged parallel to the metal surface. These calculations provide a consistent microscopic picture of ions and water throughout a double layer including the species next to the charged surface, in the 'diffuse layer' and in the bulk zone. The effect of finite size of ions and water are clearly evident, as is the effect of the large electric field on the orientation of surface water molecules.

In the calculations reported here the simulation cell has edge length 3.724 nm, with a flat metal plate at $z = 1.862$ nm and a flat restraining wall at $z = -1.862$ nm. The cell contains between 1400 to 1600 water molecules and the NaCl concentration is 1M, 2M or 3M. The electric charge density on the flat metal plate is either -9 or -18 Cm^{-2}.

The calculations show that a diffuse layer is formed between the metal and the region of the cell that acts like a bulk electrolyte zone. The ions in the diffuse layer shield the metal charge so that there is no field in the bulk electrolyte zone which is locally approximately neutral. In all previous papers in which molecular dynamics or Monte Carlo simulations of the adsorption of ions on electrodes were considered, there was no demonstration of the simultaneous existence of a diffuse layer and a bulk region. In other words the simulations were not on a scale to permit adsorption in the presence of an established double layer. We believe this is a prerequisite for all calculations to correctly describe the local and global properties of the electric double layer. In all the calculations reported here we use the SPCE water model [1] (three charged ($q_H = 0.4238e$) mass points, bond angle 109.5°, OH bond length 0.1 nm, inside a Lennard-Jones sphere with radius $\sigma = 0.317$ nm and well depth $\varepsilon = 0.650$ kJ/mole) and associated parameters for NaCl[2].

In an attempt to reduce the amount of computer time we use the immersed electrode model[3-5] for a film of electrolyte on a charged metal surface. This approach is useful because it reduces the number of water molecules in the calculation, and because there is only one metal surface (always shown on the rhs in the figures) there are no multiple images in the calculation of electric fields and potentials. In the immersed electrode model the charge on the metal is defined by and completely screened by the
excess charge in the aqueous subphase. It therefore mimics what happens in larger systems. In all previous simulations the number of ions was too small for there to be an identifiable bulk region [3-7]. This turns out not to be the case in the present set of calculations.

The metal was modelled by two linearly superimposed potentials. Pauli repulsion and dispersive attractive interactions were modelled by a 9-3 potential, of the type used by Lee et al[8]. The atom-surface interaction parameters describing interaction with nonconduction electrons were

chosen to be the same as those used by Lee at al[8]. The interactions between ions and water and the conduction electrons was modelled by their respective image potentials.

In the calculations described here the image plane and origin plane of the 9-3 potential were coincident. This was tantamount to choosing the image plane and the nuclear plane of the metal surface to be coincident. This was acceptable in our scheme because the Lennard-Jones core parameters σ are all large and the 'thickness' of the repulsive wall is also large (ca. 0.247 nm). The calculation of the image fields was done very accurately using a code based on the fast multipole method (fmm) and using the physically correct boundary conditions for a system with one metal surface. Neither the direct long range coulomb interaction nor the image interaction were cut off at a finite distances. The fast multipole method developed by Greengard and Rokhlin [9-12] is of order N in the number of charged particles in the system. It is the only viable method for large simulations like the one described here.

Finally some comments on screening of charged surfaces. At high salt concentrations the region with excess ionic charge is microscopically small. A rough estimate of the thickness of the zone in which screening occurs, valid for dilute solutions (< 0.1 M), is given by $d = \kappa^{-1}$ the inverse of the Debye-Hückel screening constant[13]

$$d = \sqrt{\left(\frac{\epsilon kT}{8\pi e^2 n_b v^2} \right)}$$

[1]

Here ϵ is the macroscopic dielectric constant of the solvent (approximately 80 for water), v the valence of the ion (always magnitude one in this paper), and n_b is the bulk concentration of the ions. Typical values of d are: 9.6 nm for 0.001 M, 3.1 nm for 0.01 M, 0.96 nm for 0.1 M, 0.31 nm for 1.0 M, and 0.18 nm for 3 M NaCl solutions. Obviously in high salt concentrations the screening should be more efficient and the screening length smaller, but since the numbers are smaller than the diameter of a water molecule it is not clear if they have any real meaning out of the plane. At high concentrations there are in fact a myriad of difficulties with simple Gouy-Chapman theory[14-16] and many modifications to the theory have been proposed[13]. There are three main problems: first the dielectric constant of water, second the finite size of ions and solvent which represent the lower length scale, and third correlated motion amongst ions and water. For example there is no reason to believe that the appropriate value of ϵ, the dielectric constant of water, is 80 near a surface or in a high electric field where dielectric saturation can occur. This subject has been discussed many times in the electrochemical literature[17]. Therefore we can only take the theoretical values of screening lengths for concentrated solutions as an rough measure of double layer thickness, and should be especially cautious when d is smaller than the size of an ion or solvent molecule.

SCREENING IN SPCE NaCl ELECTROLYTE

This section describes the interaction of hydrated Na^+ cations and Cl^- anions in solvent composed of SPCE water molecules with a charged metal surface. Each simulation was run for one nanosecond or longer, and the instantaneous spatial positions of all the atoms recorded every picosecond. The first 100 ps were discarded as anneal time. Then density probability functions $\rho(z)$ were constructed by averaging over the remaining time and over the x and y coordinates parallel to the metal surface to give functions of z the coordinate in the direction perpendicular to the surface. Figure 1, in particular shows the density profile results for Na^+ cations, Cl^- anions and SPCE water molecules in a 3M salt solution at a temperature of 50° C. Calculations with temperatures as high as 100° C where originally selected to improve the statistics. Temperature dependence of the probability distributions in the range 30 to 100° C is weak. In the 50° C simulation there were 94 Na ions, 86 Cl ions and 1416 water molecules. The charge on the electrode, equal to the image charge, is -(94 - 86)e or -8e, equivalent to a surface charge density of -17.77 Cm^{-2}.

The excess sodium ions, attracted to the electrode by the image charge, screen the electrode charge. The screening charge is concentrated in the peak at 1.45 nm in the sodium density on the right hand side of the simulation box near the point where the 9-3 wall potential passes through zero (z_w = 1.615 nm). The image plane of the metal is located at the extreme the right hand vertical edge of the Figure 1 at z = 1.862 nm. Simple Gouy-Chapman theory would predict an increase in charge to a finite value at the metal surface. There is no peak in simple theory because ions are point-like objects and the solvent is a continuum with a fixed dielectric constant. The peak in the cation distribution at z = 1.45 nm is a consequence of a finite ion radius and the hydration of the ions. The solvent layer at the electrode also effects the position and shape of the cation distribution near the metal. Note that for $|z| < 1.0$ nm the cation distribution is approximately flat at 30 ions nm^{-1}. There is also a small peak on the left hand side at ca. $z = -1.4$ nm, that is not associated with screening but is instead due to layering of the water molecules at the flat restraining wall. This wall potential goes through zero at z = -1.615 nm. Note that the chloride ion distribution does not show a peak in the same region as the cation peak because negative ions are repulsed by the negatively charged metal electrode.

The chloride probability distribution has no major structural features, certainly no peak like the screening peak at z = 1.45 nm in the Na^+ distribution. Starting from the metal on the right side of Figure 1, the chloride ion distribution rises to a rough plateau that stretches from z = 1.00 nm to z = -1.00 nm. The chloride and sodium ion probabilities are sufficiently similar across the plateau region for us to propose that this has the properties of a bulk zone. This suggestion is supported by the observation of approximate local charge neutrality (ion densities are the same), and very nearly equal integrated densities shown in Figure 2 for each of the concentrations at which the calculations were performed. The integrated density plots all monotonically increase with z from left to right. The initial slopes for z < -1.0 nm are less because of the rise in ion densities from zero at z = -1.615 nm to 'bulk' values for z > -1.0 nm. The solid line is the integrated density for the Na^+ ion and the dash line is for the Cl^- ions. Since the integrated

4

densities are very similar this means that the electric field is locally very small or zero in the bulk zone defined by $|z| < 1.0$ nm.

Whereas on the basis of one simulation we cannot interpret any of the minor features in the ion profiles, comparison of the three sets in Figure 2 shows the persistence of smaller features near 1.2 nm and 1.4 nm for both ions. We will discuss these features below.

The water density profile shown in Figure 1 displays well pronounced oscillations on both sides of the simulation cell due to the presence of the walls at $|z| = 1.862$ nm. Recall that the 9 - 3 wall potential is the same on both sides. The metal side (right) is distinguished by the existence of the image plane. On the metal side at z = 1.615 nm the water density peak is the strongest feature in the system due to localized water next to the metal. The surface electric field reaches its highest value in this region and water is localized as a result of its interaction with the surface field. In this simulation the waters in the first layer are oriented by this strong field and some H bonds to the bulk region are broken. This electric field effect is distinct from localization of water on Pt(100) and Pt(111) surfaces in the simulations of Heinzinger and Spohr[18], and Berkowitz[19, 20]. In these later works the localization is at top sites of the Pt surface due to directed features in the weak chemisorptive potential.

In Figure 2 we show the results of calculations that show the dependence of the ion densities on salt concentration and electrode charge. The 30° C temperature for the 2M and 1M plots was chosen because there did not appear to be a significant improvement in statistics in the earlier 50° C 3M calculation. Each calculation took approximately 3 months on a work station 80 to 90% dedicated to these calculations so it was not possible to run all the calculations at the same temperature. In these plots the Cl density has been smoothed to distinguish it from the Na ion density. Top panel displays the 3M result of Figure 1 in which there were 94 Na ions, 86 Cl ions and 1416 water molecules at 100°C, and the image charge on the electrode is -(94 - 86)e = -8e. The temperature is 50°C. Note the similarity in ion densities between -1.0 and 1.0 nm in all three examples. The middle panel displays the 2M result in which there were 62 Na ions, 58 Cl ions and 1516 water molecules, and the image charge on the electrode is -4e. The temperature is 30°C. The bottom panel displays the 1M result in which there were 32 Na ions, 28 Cl ions and 1576 water molecules, and the image charge on the electrode is again -4e. The temperature is 30° C.

In each panel the cation and anion concentrations are approximately the same for $|z| < 1.0$ nm. This identifies the region of the system with bulk electrolyte properties. Also for each system we show the integrated ion density vs distance z. The integrals are taken from z = - 1.862 nm to z = 1.862 nm., Solid line for the cation and dash line for the anion. Detailed examination shows that in each case for $|z| < 1.0$ nm the integrals are almost indistinguishable. This indicates that the electric field due to the ions is almost zero across the film as expected for a bulk electrolyte.

In each case studied the width of the electric double layer region is small but finite. As an estimate of diffuse layer width we measure from the position of the hard wall (z = 1.615 nm) to the point where the difference in integrated ion densities is 0.35 of the difference at the metal (either 8 for 3M or 4 for 1M or 2M). We can compare this with the Debye-Hückel screening

length since this is a e[-1] measure of diffuse layer thickness in the linearized form of the Gouy-Chapman theory (numbers in parentheses). For the three solutions the measures are: for 3M it is 0.2 nm (0.18 nm), for 2M it is 0.4 nm (0.24 nm), for 1M it is 0.5 nm (0.31 nm). The numbers in parentheses are the Debye shielding lengths calculated using Eqn(1). The estimates based on the ion probability distributions must be regarded as very rough because of the manner they were done. They may change when the simulations are run longer, and are very sensitive to structure in the water layers near the metal. In reality there must be effects due to the finite size of water molecules and ions, and effects due to saturation of molecular polarizability in high electric fields. However there is general agreement in trend and magnitude. This agreement would be lost if the dielectric constant for water were taken to be $\varepsilon = 6$, a value more appropriate for a zone in which the dielectric properties of water are at saturation values[17].

Returning to the topic of fine structure in the ion density profiles we note that on the metal side all the chloride distributions have two weak features at ca. 1.2 and 1.4 nm. Both features appear to be associated with peaks in the cation distribution and may therefore be due to contact pairs or solvent separated pairs. It should be cautioned that the SPCE model for water was not designed with high salt concentrations in mind, so the ion pairs may be more a feature of the model and not nature! This in turn implies that correlation between ions at high salt concentrations effects the distribution near the charged surface. It is interesting to note that there is no apparent association of similarly positioned ion peaks at the restraining wall on the left hand side of Figure 2.

Layering in the water distribution effects the ion distributions. Figure 1 shows a general result confirmed by more extensive simulations, namely ions avoid regions of high water density. On the metal side at right this is at $z = 1.615$ nm where the wall potential is zero, and at $z = 1.25$ nm where there is a secondary water peak. Note that the highly localized water layer next to the electrode creates a large exclusion region for ions of both signs compared to the restraining wall on the left hand side of the cell.

6

SUMMARY

This letter described the calculation of the structure of an electric double layer in a system large enough to show a bulk-like electrolyte region that occupied a significant portion of the whole simulation cell. Estimates of the width of the diffuse layer were consistently larger than the corresponding Debye-Hückel screening lengths.

The cations and anions density profiles screening the electrode was structured. In the case of cations there was a peak near 1.4 nm. For anions there was a shoulder at the same position. There no sign of similar structure near the restraining wall. Influence of solvent on both distributions near the metal interface was also noted. This simulation places no restrictions on either ion-ion or water-ion correlations, unlike the simple Gouy-Chapman theory where there is no correlation.

The water distribution showed a plane of localized water at the point where the 9 - 3 wall potential passed through zero. This localization involves preferential orientation of the water, and some evidence of up to three layers of water is evident.

ACKNOWLEDGEMENTS

REFERENCES

[1] H. J. Berendsen, J. R. Grigera, and T. P. Straatsma, J. Phys. Chem. **6269**, 6267 (1987).

[2] R. W. Impey, P. A. Madden, and I. R. McDonald, J. Phys. Chem. **87**, 5071 - 5083 (1983).

[3] J. N. Glosli and M. R. Philpott, Proceedings of the Symposium on Microscopic Models of Electrode-Electrolyte Interfaces **93-5**, 80-90 (1993).

[4] J. N. Glosli and M. R. Philpott, Proceedings of the Symposium on Microscopic Models of Electrode-Electrolyte Interfaces **93-5**, 90-103 (1993).

[5] M. R. Philpott and J. N. Glosli, Theoretical and Computational Approaches to Interface Phenomena. (1994).

[6] J. N. Glosli and M. R. Philpott, J. Chem. Phys. **96**, 6962-6969 (1992).

[7] J. N. Glosli and M. R. Philpott, J. Chem. Phys. **98**, 9995-10008 (1993).

[8] C. Y. Lee, J. A. McCammon, and P. J. Rossky, J. Chem. Phys. **80**, 4448-4455 (1984).

[9] L. F. Greengard, *The Rapid Evaluation of Potential Fields in Particle Systems*. (The MIT Press, Cambridge, Massachusetts, 1987).

[10] L. Greengard and V. Rokhlin, J. Comp. Phys. **73**, 325-348 (1987).

[11] J. Carrier, L. Greengard, and V. Rokhlin, Siam J. Sci. Stat. Comput. **9**, 669-686 (1988).

[12] L. Greengard and V. Rokhlin, Chemica Scripta **29A**, 139-144 (1989).

[13] J. Goodisman, *Electrochemistry: Theoretical Foundations* (Wiley-Interscience, New York, 1987).

[14] G. Gouy, Ann. phys. **7**, 129 (1917).

[15] D. L. Chapman, Phil. Mag. **25**, 475 (1913).

[16] J. O. Bockris and A. K. Reddy, *Modern Electrochemistry, Vol.1* (Plenum Press, New York, 1973).

[17] B. E. Conway, J. O. Bockris, and I. A. Ammar, Trans. Faraday Soc. **47**, 756 - 766 (1951).

[18] K. Heinzinger, Computer Modelling of Fluids Polymers and Solids, NATO ASI Series C **293**, 357-404 (1990).

[19] M. R. Reddy and M. Berkowitz, Chem. Phys. Letters **155**, 173-176 (1989).

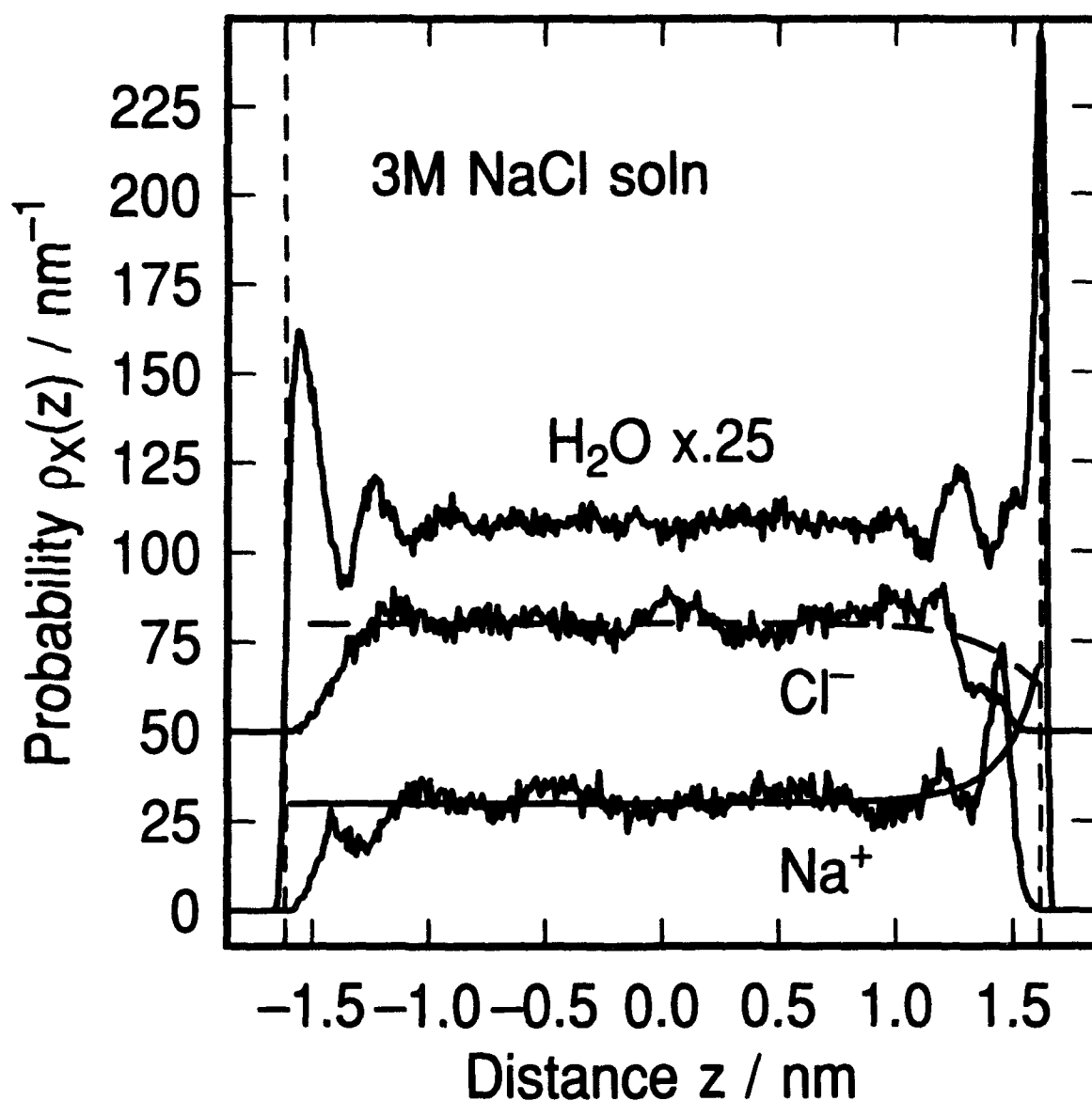[20] K. Raghavan, K. Foster, K. Motakabbir, and M. Berkowitz, J. Chem. Phys. **94**, 2110-2117 (1991).

Figure 1. Ion and water probability density distributions for 3M salt solution at 50°C, charge on the electrode q_M = -8e. Composition of the simulation cell: 94 Na$^+$ ions, 86 Cl$^-$ ions, and 1463 water molecules. Metal electrode on right hand side at z = 1.862nm (position of image plane), restraining wall origin on the left at z = -1.862 nm, positions where the wall potentials on both sides of the simulation cell go through zero at |z|= 1.615 nm are shown by vertical broken lines. Water density shows highly localized surface layer of water near z = 1.62 nm. The cation distribution shows a sharp peak near z = 1.45 nm corresponding to the excess positive ions that screen the negatively charged electrode. The Gouy-Chapman distribution for cations and anions is shown superimposed on the chloride (broken line) and sodium (solid line) ion distribution.
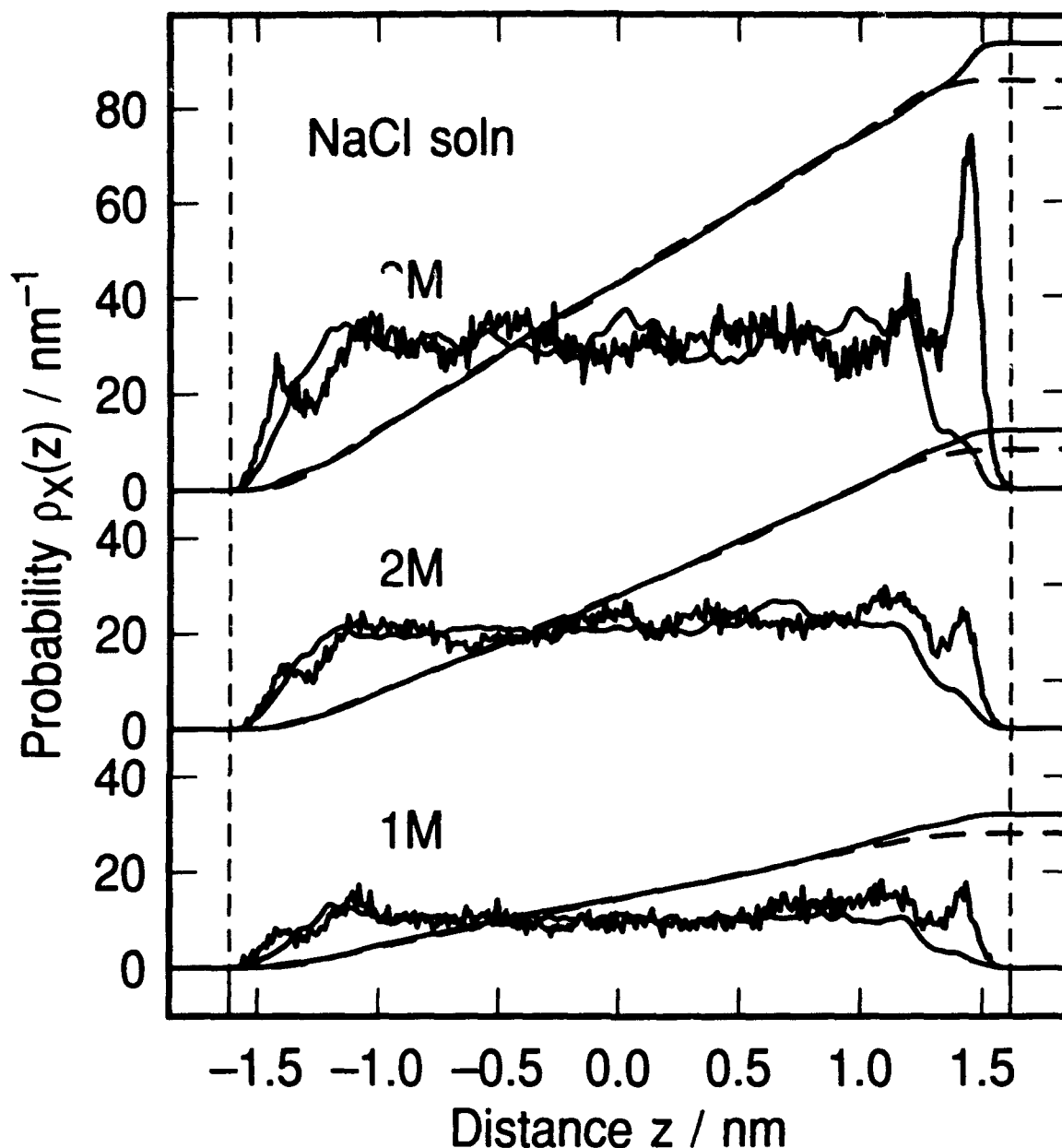
Figure 2. The sodium and chloride ion probability distributions in 3M (50°C, electrode charge -8e), 2M (30°C, electrode charge -4e), and 1M (30°C, electrode charge -4e) aqueous sodium chloride solution. Smoothed curves are for chloride, and the unsmoothed curves are for sodium cations. Metal electrode on right hand side at z = 1.862nm (position of image plane), restraining wall origin on the left at z = -1.862 nm, wall potentials on both sides of the simulation cell go through zero at lzl= 1.615 nm (shown by vertical broken lines). The integral of each ion distribution is plotted , solid line for cation dashed line for the anion. The two integrals diverge near the metal wall, where the excess cations are concentrated and shield the electrode charge. The depletion of the anion distribution has structure that is induced by layering in the water profile. Note that all the distributions show a distance dependence that deviates from the behavior expected qualitatively from the simple Gouy-Chapman theory.